A Proposed Study of Hydrogen Bond Entropic Contributions
to Chemical Carbon Capture

Jade Chongsathapornpong

MIT Climate & Sustainability Consortium, Cambridge, MA 02139

(Dated: August 29, 2022)

Hydrogen bonding interactions influence the properties of innumerable chemical systems. This work presents a brief review of their importance in chemical carbon capture. Then, considering experimental findings in the literature, we hypothesize an enhancement of cyclic CO_2 capacity which may occur in certain thermally regenerated CO_2-binding organic molecules that favor intramolecular hydrogen bonding upon CO_2 uptake. This effect, similarly to a chelate effect, might stem from the entropy penalty associated with constraints imposed by intramolecular hydrogen bonds on internal rotational degrees of freedom. Simplistic calculations are performed to estimate the magnitude of this effect in a model system. We then outline a more thorough approach with experiment and computation. The effect, if it exists, is expected to have limited applications in designing next-generation carbon capture compounds.

I. INTRODUCTION

Every year, tens of billions of tons of heat-trapping gases such as carbon dioxide enter the atmosphere. These gases should be mitigated to avoid the worst effects of climate change. Large amounts of anthropogenic CO_2 come from point sources, such as traditional fossil-fuel power plants or industrial sites. As an example of a critical industrial activity which directly coincides with CO_2 emissions, the production of cement currently involves calcination of $CaCO_3$ to CaO, inherently releasing CO_2. The cement industry accounts for around 5-7% of emissions worldwide, having emitted approximately 2 billion tons of CO_2 in 2007 [1]. There is a major economic incentive to adapt existing infrastructure to a lower-carbon future. In the oil and gas industry alone, if business-as-usual operations continue, realignment of the economy to limit global average warming to $2°C$ will result in $1.4 trillion in stranded assets [2]. Other industries which are difficult to decarbonize, such as the cement industry, may face the same costly fate. One approach to mitigating carbon emissions for such industries is carbon capture and sequestration (CCS).

Current state-of-the-art technologies in this space were developed in the 1930s [3]. They involve amines, such as monoethanolamine, which react in aqueous solution with carbon dioxide to form carbamates. These are later heated to release the CO_2 and regenerate the amines [4]. This incurs a sizable energy cost, exceeding 20% of total power for many power plants. As regeneration often occurs above $110°C$, integration with a steam cycle or construction of an entirely separate steam generator is typically needed to facilitate heating. This leads to large capital costs in retrofitting point sources with existing amine carbon capture equipment [5]. To make matters worse, many carbon capture chemicals suffer from degradation, in some real-world tests over 0.5 mol % per day [6], and can produce environmentally toxic decay products. These factors contribute to the glacial pace of CCS deployment. According to the IEA, worldwide CCS capacity is roughly 40 Mt/year—current targets for decarbonization, which already include a 90% reduction in baseline global CO_2 emissions by 2050, will require a further 7,600 Mt/year of CCS.

The past decade has seen renewed interest in carbon capture system design and innovation. Diverse electrochemical [5, 7–9] and physical [10, 11] schemes have been developed, offering useful trade-offs and improvements over standard amine approaches. Within thermally-regenerated chemical scrubbing, a litany of new systems have emerged. Solid diamine-appended metal-organic frameworks promise a new range of performance characteristics and are beginning to see commercial use [12]. Various methods of achieving phase separation on CO_2 binding lead to improved regeneration efficiency and temperature swing requirements [13–15] or allow only non-toxic amino acids to be exposed to atmosphere [16]. Neat CO_2-binding organic liquids which can benefit from polarity swing assisted regeneration show some promise [17]. Recently, covalent organic frameworks incorporating N-heterocyclic carbenes for CO_2 binding have been demonstrated, which represent new chemical design space to explore [18].

As part of our broader efforts to generate and assess candidates for next-generation capture chemicals, we would like to explore perhaps lesser-known design principles. Some experimental results hint at entropic effects which to our knowledge are not discussed in the chemical carbon capture literature. Explored in this article is a
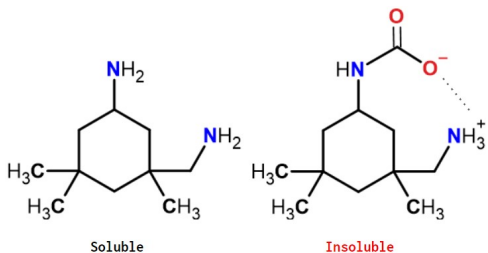
FIG. 1. Liquid isophorone diamine (left), forms a solid carbamic acid precipitate when CO_2 is bound. Of compounds in [15], monoamines did not precipitate, while diamines with suitable geometries for cooperative intramolecular hydrogen bond interactions (right) tended to form precipitates.

FIG. 2. Pair of alkanolguanidines from [19]. The molecule with 6-carbon chain absorbs significantly more CO_2.

potential chemical design space in which the temperature swings required to thermally regenerate carbon capture compounds are reduced by considering entropic effects.

II. DISCUSSION

A. Hypothesis

The research groups of Heldebrant and others have shown certain molecules preferentially form intramolecular hydrogen bond structures when CO_2 is bound, and that the relative incidence of intra- versus intermolecular hydrogen bonding can have strong implications for physical properties like viscosity [19–22].

Perhaps hydrogen bond effects are more widespread. For example, they might account for the solubility changes observed in [15] due to CO_2 hydrogen bonding occupying sites which would otherwise permit interaction with other absorbent molecules, as shown in Fig. 1. Here we focus on another intriguing prospect, the directed use of intramolecular hydrogen bonds to magnify the entropy change of CO_2 binding/release.

Our proposition is straightforward: chemicals which capture CO_2 in a thermal cycle use the temperature-dependence of spontaneity of CO_2 release (or, conversely, binding), which is quantified by the Gibbs energy $\Delta G = \Delta H - T\Delta S$, negative quantities indicating spontaneous reactions. At lower temperatures, the equilibrium is such that most CO_2 in the system is bound, while at higher temperatures this equilibrium is shifted toward free CO_2. This is chiefly an entropy-driven process; releasing CO_2 is endothermic, favoring the bound state, while free CO_2 is of higher entropy, favoring the free state. If the entropy change ΔS associated with CO_2 binding/release is magnified, all else held equal, a smaller temperature swing cycle can effect the same change in ΔG, which in turn gives the same change in equilibrium constant, and there-
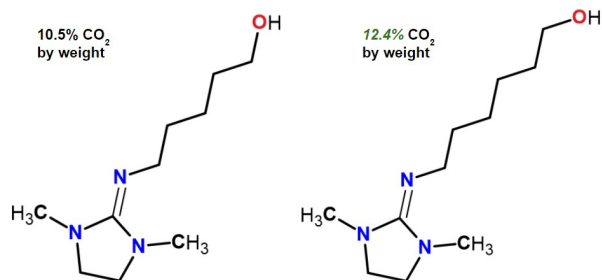
fore the same cyclic capacity. This entropy change between CO_2-bound and free states might be magnified by formation of intramolecular hydrogen bonds which constrain an initially flexible structure.

B. Observations

There are several works from which lessons can be drawn. To begin, we sought out studies of molecules with hydrogen bonding functionality on a flexible substituent.

1. Alkanolguanidines

Guanidines are strong bases which have attracted attention in recent years for their ability to bind CO_2. Molecular dynamics and experimental studies indicate that substituent structure dramatically influences the hydrogen bonding behavior of alkanolguanidines, in some cases producing order-of-magnitude changes in the extent of intramolecular hydrogen bond formation, to which large changes in viscosity are attributed [23].

In part of an older study by Koech et al., a series of N-heterocyclic imines was produced with varying substituents on the exocyclic nitrogen [19]. Of note are a pair with 5- and 6-carbon chains. These alkanolguanidines were otherwise identical, as shown in Fig. 2.

When evaluated for CO_2 absorption capacity, the species appended with 5-carbon alcohol was found to absorb 10.5% CO_2 by weight, corresponding to 58% conversion on a molar basis. Surprisingly, the species with 6-carbon alcohol performed significantly better, achieving 12.4% CO_2 uptake by weight or 72% molar. Our preliminary explanation is that an intramolecular hydrogen bond involving bound CO_2 can be formed with less strain in the 6-carbon case than the 5-carbon one. Under lower-temperature absorption conditions, the stability of the hydrogen-bonded state outweighs the entropic penalty of cyclization. The more enthalpically favorable binding
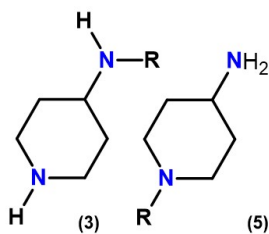
FIG. 3. Two core diamine structures denoted (**3**) and (**5**) from [24]. We focused on $\mathbf{R} = (CH_2)_n OH$, with $n = 2, 3, 6$. We noted the non-monotonic dependence on chain length of CO_2 molar cyclic capacity between 40-90°C which may be attributable to intramolecular hydrogen bonds. This non-monotonicity was similar in both structures.

would result in the observed higher uptake. Presumably, a greater entropic penalty would also be present. Unfortunately, the absorption data provided in this study, lacking measurements of cyclic capacity or temperature dependence of CO_2 solubility, is not adequate to draw firm conclusions. Detailed characterization appears missing because this series of alkanolguanidines was soon superseded in performance; further studies by the group focus on more compact molecules optimizing intramolecular hydrogen bonding, for benefits in viscosity which are critical to practical carbon capture systems [22, 23]. Regardless, the unusual performance variation with substituent chain length may suggest hydrogen bonding is at play. Revisiting these alkanolguanidines may help test the hypothesis proposed earlier.

2. Cyclic Diamines

In a survey performed by Yang et al., around 30 di- and triamines were constructed combining a set of core structures with a diverse set of substituents [24]. Among them, two series saw primary alcohol ($\mathbf{R}$) of varying length attached either to the exocyclic or cyclic nitrogen of the diamine cores depicted in Fig. 3. The compounds' cyclic CO_2 capacities between 40-90°C were measured.

For both core structures, on a molar basis compounds with 2-carbon alcohol substituents performed better than 3-carbon ones. Remarkably, this trend does not continue for longer chain lengths. For (**3**), the molar capacity of the compound with 6-carbon alcohol is comparable to that of the 2-carbon one; for (**5**), 6 carbons yields a higher capacity than 2 carbons.

To the authors, this non-monotonicity suggests a qualitative difference in how CO_2 is bound in the molecules appended with 6-carbon alcohols. That both (**3**) and (**5**) exhibit the same trend indicates the effect is a function
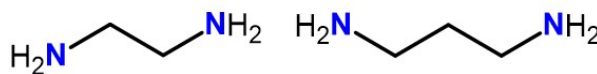

FIG. 4. Representative diamine pair from [25].

of geometry, and not the type of amine functionality involved. Intramolecular hydrogen bonding upon CO_2 capture may occur more easily with flexible 6-carbon chains than shorter, stiffer 2-carbon chains where strain perhaps offsets the otherwise favorable enthalpy of hydrogen bonding. Unfortunately, no data appears for 4- or 5-carbon chains. The enhanced cyclic capacity in the 6-carbon case could then be explained by a magnified entropy penalty from intramolecular hydrogen bonding. However, this is not the only possible explanation.

3. Linear Diamines

A follow-up study by Zhang et al. explored linear diamines pairing primary, secondary, and tertiary amine functionalities at the ends of 2- and 3-carbon chains [25]. These are interesting because they reveal a confounding variable to consider.

Density functional theory calculations suggest both 2- and 3-carbon diamines are able to form intramolecular hydrogen bonds. It is found empirically that the 3-carbon diamines generally outperformed their 2-carbon counterparts in cyclic capacity and desorption kinetics. Zhang et al. attribute this to a less stable (according to their calculations) hydrogen bonded structure in the 3-carbon cases. Their interpretation is that a strengthened hydrogen bond between the bound CO_2 and second amine group leads to a more stable carbamate zwitterion, which is less likely to form a bicarbonate. The formation of bicarbonate is associated with a 1:1 amine-to-CO_2 binding mode, whereas formation of carbamates corresponds to a lower-capacity 2:1 mode. This ostensibly accounts for higher capacity with the apparently less stable hydrogen bonding of the 3-carbon diamines.

Now we attempt to apply this explanation to [24], assuming intramolecular hydrogen bonds are important. We believe the cyclic diamine appended with 6-carbon alcohol may exhibit intramolecular hydrogen bonding, while the 3- and especially 2-carbon variants less so due to more constrained geometry. The idea of [25] that hydrogen bonding stabilizes carbamate zwitterions against hydrolysis to bicarbonate would suggest the diamines with 6-carbon alcohol, which perhaps do more hydrogen bonding, should favor a 2:1 carbamate binding mode and therefore possess inferior capacity. This is not the case.

In fact, the opposite explanation appears elsewhere: it is said intramolecular hydrogen bonds actually *destabilize* carbamate zwitterions, promoting the formation of bicarbonate in water [26]. Either the explanation of [25] is incorrect, or our assumptions about which molecules more easily form intramolecular hydrogen bonds are false.

Regardless, the formation of additional bicarbonate alone may account for observed increases in cyclic capacity, without resorting to the entropy change hypothesis. As a remark, this confounding variable should not exist in neat CO_2-binding organic liquids, such as the alkanolguanidines previously described. Unfortunately, with CO_2-rich speciation and kinetics data only available for a select few compounds in [24], this remains unclear for the cyclic diamines. Owing to the time-consuming nature of fully characterizing absorbents, it is understandable that many authors focus on their most promising candidates, which can exclude some molecules that would otherwise be informative. Moreover, it seems reports of enthalpy and entropy changes associated with CO_2 binding, which would provide the most direct information, are rare in this body of research.

C. Calculation

To justify further work, it is prudent to estimate the magnitude of the proposed effect using estimated values, to ensure it is expected to be observable. Consider an imaginary compound X which binds CO_2 in a 1:1 mode.

1. Typical Thermodynamic Values

For a ballpark estimate of typical CO_2 binding enthalpy and entropy, we turn to an article on metal-organic frameworks (MOFs). The MOF reported in [27], which is purported to be thermodynamically suited to capture from coal power plant flue gas, has a measured binding enthalpy ΔH around -70 kJ/mol, and an entropy change on binding ΔS around -200 J/mol·K. Because the mechanism involved—binding by an amine supported on a MOF—is closely related to those present in our liquid phase or aqueous compounds of interest, it is reasonable to assume we are dealing with similar values.

Our hypothesized effect stems from a greater entropic penalty for binding CO_2, arising from constraints imposed by a hydrogen bond on internal rotational degrees of freedom in an initially flexible substituent. A reasonable analogy may be the entropy of cyclization of linear molecules. For common saturated hydrocarbons, this value measured at room temperature ranges from $\Delta S =$ 32 J/mol·K for formation of a 3-carbon ring, to a maximum of 88 J/mol·K for a 6-carbon ring. We assume an intermediate value of 60 J/mol·K. In reality with the weaker hydrogen bond it is likely lower.

Hydrogen bonding of course has an enthalpic contribution. Rough estimates give O-H$\cdots$:N bond energies at -29 kJ/mol, O-H$\cdots$:O at -21 kJ/mol, and N-H$\cdots$:O at -8 kJ/mol. Any strain necessary to form the bond in a given structure will make it somewhat less energetically favorable. In the alkanolguanidines, there is another ambiguity. Although publications such as [19, 22, 28] depict CO_2 as bound to the oxygen of the hydroxy group on alcohol substituents, it is known in other cases that CO_2 can bind to the imine nitrogen [29]. The former results in an N-H$\cdots$:O hydrogen bond, while the latter would have an O-H$\cdots$:O bond. Regardless of these details, we will assume a value of -20 kJ/mol.

We assume these properties are independent of temperature. A sensitivity analysis using the extreme values on the above assumptions will follow.

2. Effects on Capacity

Under the above assumptions, we can use the Gibbs energy definition $\Delta G = \Delta H - T\Delta S$, with the non-hydrogen-bonded structure having ΔH = -70 kJ/mol and ΔS = -200 J/mol·K, while the hydrogen-bonded structure has ΔH = -90 kJ/mol and ΔS = -260 J/mol·K. This is plotted in Fig. 5, with shaded area around the hydrogen-bonded structure's curve showing the ΔG resulting from taking extreme values of hydrogen bond enthalpy and cyclization entropy (-29 kJ/mol with 32 J/mol·K, and -8 kJ/mol with 88 J/mol·K).

Between 40-90°C, for the non-hydrogen-bonded structure ΔG ranges from -7.4 kJ to +2.6 kJ. For the hydrogen-bonded structure, ΔG ranges from -8.6 kJ to +4.4 kJ. If we assume the systems equilibrate at each temperature, then $\Delta G = -RT \ln K$, where $R = 8.314$ J·K^{-1}·mol^{-1}. This leads to binding equilibrium constants K from 17.2 on absorption to 0.4 on regeneration for the former, and 27.2 to 0.2 for the latter.

If we neglect non-idealities, i.e. assuming fugacity and activity coefficients are 1, then for the 1:1 CO_2 binding reaction with our compound X we have the scheme

$$X_{(aq)} + CO_{2(g)} \rightleftharpoons X \cdot CO_{2(aq)}$$
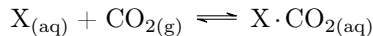
with equilibrium constant

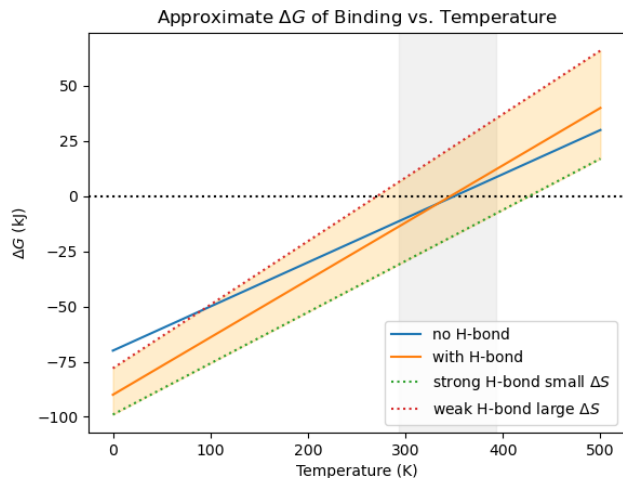$$K = \frac{[X \cdot CO_2]}{P_{CO_2} [X]}$$

FIG. 5. Plot of Gibbs energy change ΔG associated with CO_2 binding, for low (blue) and high (orange) entropy changes ΔS. The full range of possible curves based on extreme estimates of thermodynamic values is shaded orange. A typical temperature swing range is in gray.

which, if we absorb from 15% CO_2, then desorb into pure CO_2, all at 1 bar pressure, substituting into the above we can obtain the CO_2 loadings under each condition.

Conditions	mol CO_2/mol X
40°C, $K = 17.2$, $P_{CO_2} = 0.15$	0.72
90°C, $K = 0.4$, $P_{CO_2} = 1.00$	0.28
40°C, $K = 27.2$, $P_{CO_2} = 0.15$	0.80
90°C, $K = 0.2$, $P_{CO_2} = 1.00$	0.17

This gives a cyclic capacity of 0.44 mol CO_2/mol X without hydrogen bonds, and 0.63 mol CO_2/mol X with. We should be careful, though. Sensitivity of the cyclic capacity to the enthalpy and entropy changes of binding is shown in Fig. 6 and 7. At the extremes (ΔH, ΔS = -29 kJ/mol, 32 J/mol·K, or -8 kJ/mol, 88 J/mol·K, respectively) capacity *decreases*. Regardless, the takeaway is that we can expect a measurable effect from rigidization by intramolecular hydrogen bonding, and the likely parameters lead to significantly increased capacity.

III. PROPOSAL

The hypothesized effect may be consistent with the disproportionately large change in absorption capacity resulting from a structural change in alkanolguanidines, and the non-monotonic trends in cyclic diamine cyclic capacity. However, as made clear by competing explanations for diamine performance, more work is needed.
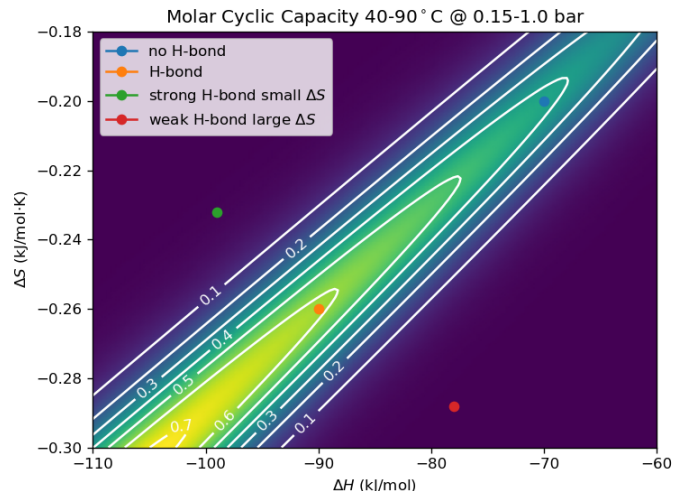

FIG. 6. Plot showing the sensitivity of cyclic capacity to the ΔH and ΔS of binding. Points corresponding to our estimated and extreme parameters for binding to X are plotted.
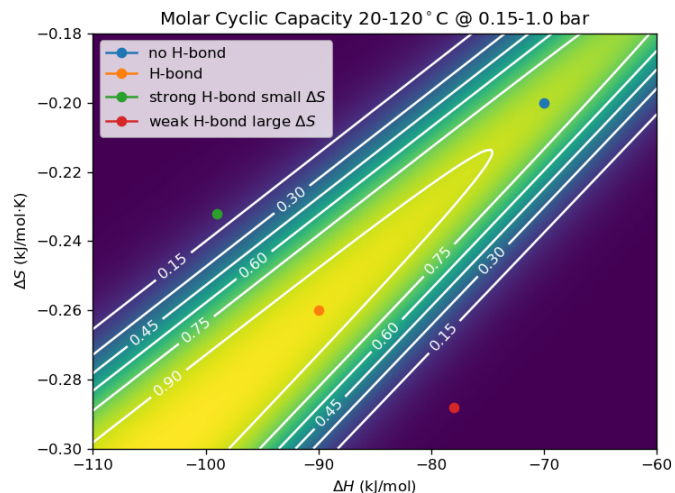

FIG. 7. Cyclic capacity sensitivity plot for compound X with wider temperature swing, under same pressures as Fig. 6.

We believe alkanolguanidines (Fig. 2) are reasonable candidates to study. Their synthesis is versatile, and they are suited to CO_2 absorption without water—therefore mitigating the confounding variable of bicarbonate formation. Our initial exploration would begin by varying the chain length of their alcohol substituents.

Ideally, our experiments would isolate intramolecular hydrogen bonding. There is no clear way to selectively switch molecules' intramolecular hydrogen bonding without side effects, so control experiments are a challenge. Computation may be useful in interpreting results, in addition to highlighting molecules of interest.

A. Computational

The computational effort would seek series of molecules which differ in how much intramolecular hydrogen bonding occurs when CO_2 is bound, but with minimal differences in how they would otherwise bind CO_2 without intramolecular hydrogen bonding. Their structure should require intramolecular hydrogen bonds to constrain internal degrees of freedom, and therefore incur an entropic penalty. A positive experimental result would see an increase in cyclic capacity for molecules which do more intramolecular hydrogen bonds, compared to ones which do less, accounting for differences in how they would bind CO_2 without those hydrogen bonds, obtained by computation. We do not have computational expertise, so this portion of the proposal should be expanded and corrected by someone more knowledgeable in the field.

1. Intramolecular Hydrogen Bond Enthalpy

Effects of substituent chain lengths on the energetics of intramolecular hydrogen bonding in molecules like Fig. 2 or 3 are where we imagine starting. Importantly, we expect that changing this chain length should not severely affect the molecules' electronic structure, and therefore should not severely change how they would bind CO_2 in the absence of intramolecular hydrogen bonds. Our impression is that changing chain lengths would make intramolecular hydrogen bonds more or less favorable, by changing the strain energy associated with hydrogen bond formation. To validate this idea, one possibility is to assume a given molecule has an intramolecular hydrogen bonded CO_2-bound conformer, then perform energy minimization making use of density functional theory. It should be possible to compare the resulting energy with a conformer lacking a hydrogen bond, to estimate the enthalpy of forming the hydrogen bond. It may also be insightful to visualize the local strain energy distribution of the molecules [30].

2. Molecular Dynamics

Molecular dynamics simulations of ensembles of molecules should also be performed to estimate the frequencies of intra- and intermolecular hydrogen bonding in our compounds of interest as CO_2 is absorbed. A methodology for conducting and interpreting such simulations is described in [28]. We would expect results to qualitatively match findings from energy minimization.

B. Experimental

Informed by computation, next we would synthesize and characterize alkanolguanidines with the chosen chain lengths. As an initial guess, we would choose 3, 4, 5, and 6-carbon alcohol substituents.

1. Synthesis of Alkanolguanidines

First, 2-chloro-1,3-dimethylimidazolium chloride is to be prepared according to procedures adapted from [31]. A Schlenk flask is flame-dried under vacuum. After allowing to cool and backfilling with inert gas, 20 g (175.2 mmol) of 1,3-dimethylimidazolidinone is added, followed by dry toluene (estimated 400 mL, but less may be possible) with stirring at room temperature. Using a dropping funnel, 26.6 g (209.6 mmol) of oxalyl chloride is added dropwise. The solution is then refluxed at 70°C for 4 hours. The product should be a solid. The solvent may be filtered via cannula, then the solid product washed with diethyl ether before being dried under vacuum. The expected yield is around 27 g (160 mmol).

Second, a protected version of the substituent is prepared from the corresponding alkanolamine, with the hydroxyl group becoming a trimethylsilyl ether. This can be done by reaction of alkanolamines with chlorotrimethylsilane or hexamethyldisilazane in the presence of auxiliary base such as triethylamine.

Third, the protected substituent and chloride salt are combined, following procedures adapted from [19]. Two flame-dried Schlenk flasks are set up. To the first, under inert atmosphere, 200 mL of dichloromethane and 165 mL (1180 mmol) of triethylamine are added, followed by 590 mmol of the chosen trimethylsilyl-protected amine. To the second, also under inert atmosphere, 200 mL of dichloromethane, and 100 g (590 mmol) of the previously prepared imidazolium chloride salt is dissolved with stirring. The resulting solution is added to the first flask dropwise via dropping funnel, at 0°C. After the addition, the flask is brought to 25°C and stirred for 72 hours.

The product should be in the liquid phase; solvent volume may be reduced by rotary evaporation. The reaction should no longer be air sensitive. The remaining liquid should be washed 3 times with 100 mL of 30% aqueous KOH, noting the product should remain in the organic fraction. The organic fraction is then dried with $MgSO_4$. After filtering off the $MgSO_4$, rotary evaporation is used again, followed by purification via vacuum distillation.

Finally, 450 mmol (approximately 120g, depending on the alkanolguanidine target) of the product of the previous stage is dissolved in methanol (estimated 500mL,

but less may be possible), then stirred with 68.2 g (490 mmol) of K_2CO_3 at room temperature for 1 hour. Filtering off solid, then using rotary evaporation to remove methanol and purifying with vacuum distillation should give the liquid product in 51% yield, about 50 g.

2. Cyclic Capacity Measurements

Although measurements of properties like absorption and desorption kinetics, heat capacity, viscosity, and vapor pressure are important to real-world applications, the effect should manifest in equilibrium CO_2 cyclic capacity alone. We are interested in CO_2 absorption isotherms, sometimes called CO_2 solubilities. These relate the CO_2 loading—for our purposes, on a molar basis—of our liquids to CO_2 partial pressures at fixed temperatures. One approach involves a sealed stirred cell of sample in a heat bath, initially filled with nitrogen, then injecting a known amount of CO_2 at the same temperature. The amount of CO_2 introduced must be known precisely; one article suggests assuming the Peng-Robinson equation of state applies, and using it to deduce the CO_2 amount from initial and final pressures and temperatures of the gas phase after injection. Gas chromatography may provide a more accurate measurement [32]. Gas and liquid phases will need time to equilibrate, as the varying degree of intermolecular hydrogen bonding in our compounds is expected to have major effects on viscosity, which affects rates. After equilibration, the headspace of the stirred cell could be sampled again by gas chromatography, to estimate the remaining CO_2 partial pressure and the corresponding amount of CO_2 absorbed. An aliquot of the liquid phase could be taken for another estimate of CO_2 loading by quantitative NMR. This process should be repeated, adding CO_2 to move to higher pressures.

Repeating that entire process at 10°C intervals yields a collection of isotherms which can be fitted to the Clausius-Clapeyron relation to estimate enthalpy and entropy changes for the transition of CO_2 from the gas phase to a condensed phase [27, 33]. The isotherms also provide cyclic capacity information, extrapolated to arbitrary temperature ranges. Corroborating with computational results, we should be able to draw conclusions.

IV. OUTLOOK

There are various considerations for committing to this project, primarily the applicability of the results. Although a positive result would suggest molar cyclic capacities can be improved by combining flexibility and directed hydrogen bonds into carbon capture molecules, this generally requires more atoms, which reduces gravimetric cyclic capacity. As the latter capacity is more significant for practical application, it's possible that this design principle would not yield fruitful gains. On the side of reducing temperature swing sizes, other technologies already offer rather small temperature swings. For example, polarity-swing assisted regeneration with CO_2-binding organic liquids can theoretically yield a 25°C swing, at the cost of later needing to separate antisolvent from the liquid [17]. Phase-change systems, which are presumably accompanied by magnified entropy penalties like our intramolecular hydrogen bonding effect would provide, also already give small temperature swings, for instance desorption at 60°C with absorption at room temperature [15], but with the added benefit of exclusively heating material which has bound CO_2. Regardless, we're interested in this effect; fundamental understanding may enable unforeseen applications.

[1] L. Barcelo, J. Kline, G. Walenta, and E. Gartner, Cement and carbon emissions, Materials and Structures **47**, 1055 (2013).

[2] G. Semieniuk, P. B. Holden, J.-F. Mercure, P. Salas, H. Pollitt, K. Jobson, P. Vercoulen, U. Chewpreecha, N. R. Edwards, and J. E. Viñuales, Stranded fossil-fuel assets translate to major losses for investors in advanced economies, Nature Climate Change **12**, 532 (2022).

[3] G. T. Rochelle, Amine scrubbing for co2 capture, Science **325**, 1652 (2009).

[4] D. J. Heldebrant, P. K. Koech, R. Rousseau, V.-A. Glezakou, D. Cantu, D. Malhotra, F. Zheng, G. Whyatt, C. J. Freeman, and M. D. Bearden, Are water-lean solvent systems viable for post-combustion CO2 capture?, Energy Procedia **114**, 756 (2017).

[5] M. Wang, H. J. Herzog, and T. A. Hatton, CO2 capture using electrochemically mediated amine regeneration, Industrial & Engineering Chemistry Research **59**, 7087 (2020).

[6] R. Idem, M. Wilson, P. Tontiwachwuthikul, A. Chakma, A. Veawab, A. Aroonwilas, and D. Gelowitz, Pilot plant studies of the CO2 capture performance of aqueous MEA and mixed MEA/MDEA solvents at the university of regina development plant and boundary dam CO2 capture demonstration plant, Industrial & Engineering Chemistry Research **45**, 2414 (2005).

[7] S. Jin, M. Wu, Y. Jing, R. G. Gordon, and M. J. Aziz, Low energy carbon capture via electrochemically induced pH swing with electrochemical rebalancing, Nature Communications **13**, 10.1038/s41467-022-29791-7 (2022).

[8] H. Seo, M. Rahimi, and T. A. Hatton, Electrochemical carbon dioxide capture and release with a redox-active amine, Journal of the American Chemical Society **144**, 2164 (2022).

[9] J. S. Kang, S. Kim, and T. A. Hatton, Redox-responsive sorbents and mediators for electrochemically based CO2 capture, Current Opinion in Green and Sustainable Chemistry **31**, 100504 (2021).

[10] S. Kumar, R. Srivastava, and J. Koh, Utilization of zeolites as CO2 capturing agents: Advances and future perspectives, Journal of CO2 Utilization **41**, 101251 (2020).

[11] L. Legrand, O. Schaetzle, R. C. F. de Kler, and H. V. M. Hamelers, Solvent-free CO2 capture using membrane capacitive deionization, Environmental Science & Technology **52**, 9478 (2018).

[12] B. Dinakar, A. C. Forse, H. Z. H. Jiang, Z. Zhu, J.-H. Lee, E. J. Kim, S. T. Parker, C. J. Pollak, R. L. Siegelman, P. J. Milner, J. A. Reimer, and J. R. Long, Overcoming metastable co2 adsorption in a bulky diamine-appended metal organic framework, Journal of the American Chemical Society **143**, 15258 (2021).

[13] D. Malhotra, J. P. Page, M. E. Bowden, A. Karkamkar, D. J. Heldebrant, V.-A. Glezakou, R. Rousseau, and P. K. Koech, Phase-change aminopyridines as carbon dioxide capture solvents, Industrial & Engineering Chemistry Research **56**, 7534 (2017).

[14] H. Machida, T. Esaki, K. Oba, T. Tomikawa, T. Yamaguchi, and H. Horizoe, Phase separation solvent for CO2 capture, Energy Procedia **114**, 823 (2017).

[15] S. Kikkawa, K. Amamoto, Y. Fujiki, J. Hirayama, G. Kato, H. Miura, T. Shishido, and S. Yamazoe, Direct air capture of CO2 using a liquid amine–solid carbamic acid phase-separation system using diamines bearing an aminocyclohexyl group, ACS Environmental Au 10.1021/acsenvironau.1c00065 (2022).

[16] R. Custelcean, K. A. Garrabrant, P. Agullo, and N. J. Williams, Direct air capture of CO2 with aqueous peptides and crystalline guanidines, Cell Reports Physical Science **2**, 100385 (2021).

[17] D. Heldebrant, *CO2 Binding Organic Liquids Gas Capture with Polarity Swing Assisted Regeneration*, Tech. Rep. (2014).

[18] C. He, D.-H. Si, Y.-B. Huang, and R. Cao, A CO2-masked carbene functionalized covalent organic framework for highly efficient carbon dioxide conversion, Angewandte Chemie International Edition 10.1002/anie.202207478 (2022).

[19] P. K. Koech, J. Zhang, I. V. Kutnyakov, L. Cosimbescu, S.-J. Lee, M. E. Bowden, T. D. Smurthwaite, and D. J. Heldebrant, Alkanolguanidine and alkanolamidine liquids for CO2 capture, RSC Adv. **3**, 566 (2013).

[20] Q.-Q. Wang, V. W. Day, and K. Bowman-James, Macrocyclic influences in co2 uptake and stabilization, Organic Letters **16**, 3982 (2014).

[21] X. Y. Luo, X. Fan, G. L. Shi, H. R. Li, and C. M. Wang, Decreasing the viscosity in CO2 capture by amino-functionalized ionic liquids through the formation of intramolecular hydrogen bond, The Journal of Physical Chemistry B **120**, 2807 (2016).

[22] D. Malhotra, D. C. Cantu, P. K. Koech, D. J. Heldebrant, A. Karkamkar, F. Zheng, M. D. Bearden, R. Rousseau, and V.-A. Glezakou, Directed hydrogen bond placement: Low viscosity amine solvents for CO2 capture, ACS Sustainable Chemistry & Engineering **7**, 7535 (2019).

[23] D. Malhotra, P. K. Koech, D. J. Heldebrant, D. C. Cantu, F. Zheng, V.-A. Glezakou, and R. Rousseau, Reinventing design principles for developing low-viscosity carbon dioxide-binding organic liquids for flue gas clean up, ChemSusChem **10**, 636 (2017).

[24] Q. Yang, G. Puxty, S. James, M. Bown, P. Feron, and W. Conway, Toward intelligent CO2 capture solvent design through experimental solvent development and amine synthesis, Energy & Fuels **30**, 7503 (2016).

[25] R. Zhang, Q. Yang, Z. Liang, G. Puxty, R. J. Mulder, J. E. Cosgriff, H. Yu, X. Yang, and Y. Xue, Toward efficient CO2 capture solvent design by analyzing the effect of chain lengths and amino types to the absorption capacity, bicarbonate/carbamate, and cyclic capacity, Energy & Fuels **31**, 11099 (2017).

[26] G. Puxty, R. Rowland, A. Allport, Q. Yang, M. Bown, R. Burns, M. Maeder, and M. Attalla, Carbon dioxide postcombustion capture: A novel screening study of the carbon dioxide absorption performance of 76 amines, Environmental Science & Technology **43**, 6427 (2009).

[27] P. J. Milner, R. L. Siegelman, A. C. Forse, M. I. Gonzalez, T. Runčevski, J. D. Martell, J. A. Reimer, and J. R. Long, A diaminopropane-appended metal–organic framework enabling efficient CO2 capture from coal flue gas via a mixed adsorption mechanism, Journal of the American Chemical Society **139**, 13541 (2017).

[28] D. C. Cantu, J. Lee, M.-S. Lee, D. J. Heldebrant, P. K. Koech, C. J. Freeman, R. Rousseau, and V.-A. Glezakou, Dynamic acid/base equilibrium in single component switchable ionic liquids and consequences, The Journal of Physical Chemistry Letters **7**, 1646 (2016).

[29] L. F. B. Wilm, T. Eder, C. Mück-Lichtenfeld, P. Mehlmann, M. Wünsche, F. Buß, and F. Dielmann, Reversible co2 fixation by n-heterocyclic imines forming water-stable zwitterionic nitrogen-base–co2 adducts, Green Chemistry **21**, 640 (2019).

[30] C. E. Colwell, T. W. Price, T. Stauch, and R. Jasti, Strain visualization for strained macrocycles, Chemical Science **11**, 3923 (2020).

[31] M. Guest, R. L. Sueur, M. Pilkington, and T. Dudding, An unsymmetrical cyclopropenimine-guanidine platform for accessing strongly basic proton sponges and borondifluoride diaminonaphthalene fluorophores, Chemistry – A European Journal **26**, 8608 (2020).

[32] W. Luo, D. Guo, J. Zheng, S. Gao, and J. Chen, CO2 absorption using biphasic solvent: Blends of diethylenetriamine, sulfolane, and water, International Journal of Greenhouse Gas Control **53**, 141 (2016).

[33] A. Nuhnen and C. Janiak, A practical guide to calculate the isosteric heat/enthalpy of adsorption via adsorption isotherms in metal–organic frameworks, MOFs, Dalton Transactions **49**, 10295 (2020).